Science Bulletin 70 (2025) 3991–3996

Contents lists available at ScienceDirect

Science Bulletin

journal homepage: www.elsevier.com/locate/scib

Article

Symmetry restoration and quantum Mpemba effect in many-body localization systems

Shuo Liu [a,b,1], Hao-Kai Zhang [a,c,1], Shuai Yin [d], Shi-Xin Zhang [c,*], Hong Yao [a,*]

[a] Institute for Advanced Study, Tsinghua University, Beijing 100084, China
[b] Department of Physics, Princeton University, Princeton, NJ 08544, USA
[c] Institute of Physics, Chinese Academy of Sciences, Beijing 100190, China
[d] School of Physics, Sun Yat-sen University, Guangzhou 510275, China

ARTICLE INFO

Article history:
Received 26 May 2025
Received in revised form 28 August 2025
Accepted 29 September 2025
Available online 17 October 2025

Keywords:
Many-body localization
Quantum thermalization
Non-equilibrium dynamics
Symmetry restoration
Quantum Mpemba effect

ABSTRACT

Non-equilibrium dynamics of quantum many-body systems has attracted increasing attention owing to a variety of intriguing phenomena absent in equilibrium physics. A prominent example is the quantum Mpemba effect, where subsystem symmetry is restored more rapidly under a symmetric quench from a more asymmetric initial state. In this work, we investigate symmetry restoration and the quantum Mpemba effect in many-body localized systems for a range of initial states. We show that symmetry can still be restored in the many-body localization regime without approaching thermal equilibrium. Moreover, we demonstrate that the quantum Mpemba effect emerges universally for any tilted product state, in contrast to chaotic systems where its occurrence depends sensitively on the choice of the initial state. We further provide a theoretical analysis of symmetry restoration and the quantum Mpemba effect using an effective model for many-body localization. Overall, this paper fills an important gap in establishing a unified understanding of symmetry restoration and the quantum Mpemba effect in generic many-body systems, and it advances our understanding of many-body localization.

1. Introduction

Non-equilibrium physics harbors various counterintuitive phenomena and has attracted increasing attention. One famous example is the Mpemba effect [1], namely, hot water freezes faster than cold water under identical conditions. This effect has been identified and investigated in various classical systems [2–12] and open quantum systems [13–28]. Recently, a quantum version of the Mpemba effect in isolated systems has been proposed [29] where subsystem U(1) symmetry starting from a more asymmetric initial state can be restored faster than that from a more symmetric initial state under the quench of a symmetric Hamiltonian. As reviewed in Refs. [30,31], this novel phenomenon is dubbed the quantum Mpemba effect (QME) and has been extensively investigated in integrable systems [32–37], free dissipative systems [38,39], chaotic systems [40–45], and quantum simulator experiments [46,47]. Furthermore, the QME has also been extended to the restoration of other symmetries, including the non-Abelian SU(2) symmetry [40] and the translation symmetry [48]. More importantly, the underlying mechanisms of QME in both integrable and chaotic systems have been established attributing to the distinct charge transport properties [36] and quantum thermalization speeds [40] associated with different initial states, respectively.

On a different front, many-body localization (MBL) [49–53] is one of the most important cornerstones for non-equilibrium physics. Although there is an ongoing debate that MBL might only be a transient phenomenon as reviewed in Ref. [54] (see also Refs. [55–64]), the phenomenology of the MBL regimes within accessible finite-size systems is well-established. In the presence of sufficiently strong disorder [65,66] or quasiperiodic potentials [67], the finite-size isolated interacting system violates the eigenstate thermalization hypothesis [68–72] and exhibits various exotic behaviors, including the logarithmic spread of entanglement [73–80] and emergent local integrals of motion [81,82]. The paradigmatic MBL Hamiltonian respects the U(1) symmetry, but the interplay between symmetry restoration and MBL regime has not been studied before. A natural question that arises is whether the U(1)

* Corresponding authors.
E-mail addresses: shixinzhang@iphy.ac.cn (S.-X. Zhang), yaohong@tsinghua.edu.cn (H. Yao).
[1] These authors contributed equally to this work.

https://doi.org/10.1016/j.scib.2025.10.017
2095-9273/

symmetry can be restored in the MBL regime as the system fails to thermalize. A companion further question is whether the QME exists in the MBL regime. More importantly, a theoretical understanding of the presence or absence of symmetry restoration and QME in the MBL regime is strongly needed.

In this paper, we investigate the U(1) symmetry restoration and the associated QME starting from various tilted product states in the thermal and MBL regimes via adjusting the strength of the disorder. In the thermal regime, the QME is present and absent for the tilted ferromagnetic state and tilted Néel state respectively, similar to what has been observed in U(1)-symmetric random circuits [40,41], which can be understood through the lens of quantum thermalization. In the MBL regime, upon varying accessible system sizes, there is a tendency that the symmetry can also be restored in the thermodynamic limit, which provides a nontrivial example for the long-time evolved state that restores the symmetry but without reaching thermal equilibrium. The associated symmetry restoration timescale grows exponentially with subsystem size. More importantly, the emergence of the QME is universal in the MBL regime, independent of the choice of the initial tilted product states. In contrast, in chaotic systems, distinct types of initial states can nevertheless exhibit the same late-time behavior in symmetry-restoration dynamics, although the presence of QME remains state dependent. For instance, while both the tilted Néel state and the tilted ferromagnetic state with a middle domain wall ultimately display similar dynamical features, the QME is absent in the former but present in the latter [40]. These unexpected results in MBL systems indicate a distinct underlying mechanism compared to those in integrable and chaotic systems.

To theoretically understand the mechanism behind symmetry restoration and QME in the MBL regime, we consider the corresponding effective model based on the emergent local integrals of motion [81,82]. In the long time limit, the degrees of symmetry breaking can be analyzed analytically. The results are identical for different initial tilted product states in MBL systems and are also consistent with the results from chaotic systems starting from initial tilted ferromagnetic states. However, the results in chaotic systems with other initial states show different patterns. Consequently, MBL quench from any tilted product states and chaotic quench from tilted ferromagnetic states share similar symmetry restoration behaviors including the presence of QME while QME might be absent in chaotic quench from other tilted product states. The main results are summarized in Table 1 (See the Supplementary material for details). We further perform a direct numerical simulation and observe the QME in the symmetry restoration dynamics under the quench of the MBL effective model.

2. Materials and methods

We consider the following one-dimensional interacting Aubry-André (AA) model [67,83–93],

$$H = -J_{\text{hopping}} \sum_i \left(\sigma_i^x \sigma_{i+1}^x + \sigma_i^y \sigma_{i+1}^y\right) + V \sum_i \sigma_i^z \sigma_{i+1}^z + \sum_i W_i \sigma_i^z, \quad (1)$$

where σ_i^x, σ_i^y, and σ_i^z are the Pauli matrices at site i, J_{hopping} is the hopping strength which we set to 1 as the unit of energy, V is the strength of interaction fixed to $\frac{1}{2}$ unless otherwise specified, $W_i = W\cos(2\pi\alpha i + \phi)$ is the quasiperiodic potential with strength W, $\alpha = \frac{\sqrt{5}+1}{2}$, and ϕ is a random phase to be averaged. We use the open boundary conditions throughout the work. There is an MBL regime with large W (see the Supplementary material for details) for accessible finite-size systems. We have also investigated symmetry restoration and QME in the interacting model with random potentials [65,66,94,95], and the qualitative behaviors remain the same (see the Supplementary material for details).

Table 1
Main results of symmetry restoration and QME in MBL and chaotic systems.

Systems and initial states	Symmetry restoration	QME
MBL from any tilted product states & chaotic system from tilted ferromagnetic states	Finite-size symmetry broken crossover	Always present
Chaotic system from other tilted product states	Restoration for any θ	State-dependent

To quantify the degrees of symmetry breaking in subsystem A, we employ the entanglement asymmetry (EA) [29] which has been extensively studied as a measure of symmetry breaking in various physical contexts [96–102]. This quantity is defined as

$$\Delta S_A = S\left(\rho_{A,Q}\right) - S(\rho_A), \quad (2)$$

namely the difference between the von Neumann entropy of the reduced density matrix of subsystem A chosen as the leftmost N_A sites, ρ_A, and that of $\rho_{A,Q} = \sum_q \Pi_q \rho_A \Pi_q$ where Π_q is the projector to the charge sector with $Q_A = \sum_{i\in A}\sigma_i^z = q$, which means that $\rho_{A,Q}$ retains only the block-diagonal components of ρ_A. EA is non-negative by definition and only vanishes when ρ_A is block diagonal for the subsystem charge sectors, i.e., ρ_A is U(1) symmetric. Therefore, $\Delta S_A = 0$ is a necessary but not sufficient condition for thermal equilibrium. In the theoretical analysis, we utilize Rényi-2 EA $\Delta S_A^{(2)}$ by replacing von Neumann entropy with Rényi-2 entropy for simplicity, which shares qualitatively the same behaviors as ΔS_A and is experimentally relevant [46].

The initial states are chosen as tilted product states. Two typical initial states include tilted ferromagnetic states (TFS) and tilted Néel states (TNS):

$$|\psi_0(\theta)\rangle = \begin{cases} e^{-i\frac{\theta}{2}\sum_j \sigma_j^y} |0\rangle^{\otimes N}, & \text{TFS} \\ e^{-i\frac{\theta}{2}\sum_j \sigma_j^y} |01\rangle^{\otimes N/2}, & \text{TNS} \end{cases} \quad (3)$$

where N is the system size and θ is the tilt angle controlling the degree of the initial symmetry breaking. EA of these two types of initial states is $\Delta S_A = 0$ when $\theta = 0$ and increases monotonically with larger θ until it reaches the maximal value at $\theta = \pi/2$.

After choosing a specific initial state, the system evolves under a quench of the Hamiltonian given by Eq. (1). The reduced density matrix of subsystem A at time t is $\rho_A(t) = \text{tr}_{\overline{A}}\left(e^{-iHt}|\psi_0(\theta)\rangle\langle\psi_0(\theta)|e^{iHt}\right)$ where $\overline{A}$ is the complementary subsystem to A. We calculate the EA dynamics of subsystem A averaged over different random phases ϕ to investigate the symmetry restoration and the QME.

3. Results

We employ python packages TensorCircuit [103] and QuSpin [104,105] to perform numerical simulations, where TensorCircuit package provides a convenient method to prepare required initial states by applying quantum gates. The averaged EA dynamics with initial TFS and TNS are shown in Fig. 1a–d. We note that the qualitative behaviors are consistent for different subsystem A as long as the subsystem size $N_A < N/2$ (see the Supplementary material for details) and the subsystem symmetry in general cannot be restored when N_A exceeds half of the total system size [100].

In the thermal regime with small $W = 2.0$, as shown in Fig. 1a, c, the QME is present for the initial TFS but absent for the initial TNS. The initial state dependence of the QME in chaotic systems has been observed in the U(1)-symmetric random circuits [40,41],

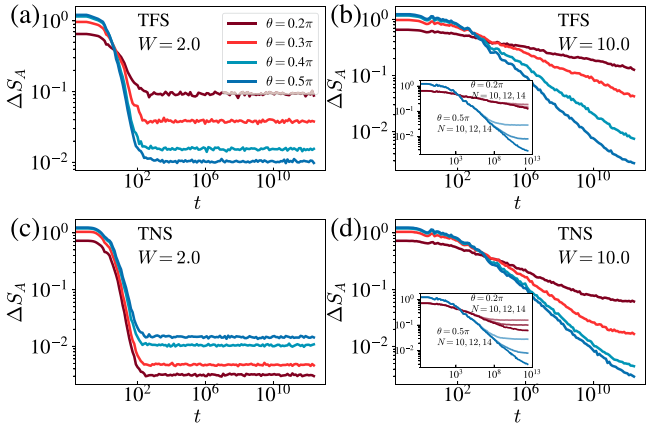

Fig. 1. EA dynamics averaged over different random phases ϕ with $N = 14$ and $N_A = 3$, i.e., subsystem $A = [1, 2, 3]$. The initial states of (a, b) and (c, d) are TFS and TNS respectively. For TFS, QME consistently appears for all values of W. For TNS, QME emerges exclusively in the MBL regime. The insets of panels (b) and (d) show the EA dynamics with fixed $N_A = 3$ and varying N. The QME remains robust with a nearly constant timescale as the total system sizes increase.

which can be understood through the lens of quantum thermalization, namely, the thermalization speed is slower in charge sectors with a smaller Hilbert-space dimension. ρ_A of the initial TFS and TNS are both symmetric with $\theta = 0$ and become more U(1) asymmetric with increasing tilt angle θ. However, when $\theta = 0$, TFS and TNS reduce to ferromagtic state $|0\rangle^{\otimes N}$ and Néel state $|01\rangle^{\otimes N/2}$ respectively. The former belongs to the smallest charge sector while the latter resides in the largest half-filling sector. Therefore, for ρ_A of TFS, the weights of the smaller charge sectors decrease as θ increases, i.e., the more asymmetric initial state has a faster thermalization speed [40]. Consequently, the QME is anticipated. On the contrary, for ρ_A of TNS, the weights of the smaller charge sectors increase with increasing θ, i.e., the more asymmetric initial state has a slower thermalization speed [40]. Therefore, the EA with a more asymmetric initial state remains larger than that with a more symmetric initial state under the quench, and thus the QME is absent.

In contrast, deep in the MBL regime with sufficiently large $W = 10.0$, QME always occurs regardless of the choice of initial states as shown in Fig. 1b, d. The symmetry restoration dynamics in the MBL regime are not only distinct from those observed in the thermal regime as discussed above but also show different late-time behaviors compared to integrable systems where symmetry cannot be restored for initial TNS [33]. This distinction further underscores the uniqueness and significance of investigating symmetry restoration and QME in the MBL regime. Moreover, although the late-time EA saturates to a nonzero value within accessible finite-size systems, it decreases as the system size increases as shown in insets in Fig. 1b, d, indicating the symmetry restoration in the thermodynamic limit.

It is worth noting that the timescale of QME, defined as the EA crossing between different tilt angles θ, in the MBL regime would increase exponentially with the subsystem size N_A due to the logarithmic lightcone [73,75–79], whereas the QME timescale in integrable and chaotic systems scales polynomially with N_A [41]. This observation is further supported by the results in the insets of Fig. 1 where the QME timescale remains unchanged for the same subsystem size and different total sizes. Although the possible deviation from logarithmic lightcone at long times with increasing system size has been reported [106], a much longer time is still required to observe the QME in the MBL regime in finite size systems, which explains the experimentally nonvisible QME in a disordered interacting system due to the constraint evolution time reached [46]. To observe QME in the current experimental platforms, we can choose a smaller subsystem size N_A. See the Supplementary material for more discussions. Moreover, it is well-known that the system in the MBL regime keeps a memory of the initial state, e.g., the non-vanishing charge imbalance starting from a Néel state. In other words, quantities such as charge imbalance for the initial tilted Néel states and the associated late time states both increase with increasing θ. The order-reversal behavior of EA associated with the QME studied in this work is not inconsistent with this memory characteristic of the MBL regime since EA is a non-local observable and the initial information is encoded in the diagonal part of the disorder averaged late-time subsystem density matrix (see the Supplementary material for details).

In the absence of the interaction ($V = 0$), the AA model enters the Anderson localized phase when $W > 2$. As shown in Fig. 2, the degree of symmetry breaking becomes frozen, and the EA remains essentially at its initial value. Therefore, both symmetry restoration and QME are absent in the Anderson localization phase. As detailed in the Supplementary material, these results can also be understood through the effective model of MBL discussed below by setting the coupling $J = 0$.

To analytically understand the distinct behaviors of symmetry restoration in the MBL regime, we consider the fully diagonalized effective model [81,82,107–110] for the MBL regime obtained under a local unitary transformation:

$$H_{\text{eff}} = \sum_i h_i \tau_i^z + \sum_{i<j} J_{ij} \tau_i^z \tau_j^z + \cdots, \tag{4}$$

where $\tau_i^z = \sigma_i^z + \sum_{j,k} \sum_{\alpha,\beta=x,y,z} c^{\alpha,\beta}(i,j,k) \sigma_j^\alpha \sigma_k^\beta + \cdots$ are local integrals of motion with c decaying exponentially with the distance between i and j, k, h_i is uniformly sampled from $[-h, h]$, and $J_{ij} = \widetilde{J}_{ij} e^{-|i-j|/\xi}$ with $\widetilde{J}_{ij} \in [-J, J]$ and ξ denoting the localization length. In the following analysis, we further approximate the effective model by replacing τ_i^z with σ_i^z and neglect the higher-order terms (see more numerical results of the effective model with higher-order terms in the Supplementary material).

We focus on the Rényi-2 EA which is experimentally relevant and given by

$$\Delta S_A^{(2)}(t) = \log \frac{\text{tr}\rho_A^2(t)}{\text{tr}\rho_{A,Q}^2(t)}. \tag{5}$$

$\rho_A(t)$ and $\rho_{A,Q}(t)$ can both be decomposed into a complete Pauli operator string basis $P^{\boldsymbol{\mu}} = \sigma_0^{\mu_0} \sigma_1^{\mu_1} \cdots \sigma_{N_A-1}^{\mu_{N_A-1}}$ where $\sigma_j^{\mu_j}$ is the μ-type operator on j-th site choosing from $\left\{I_j, \sigma_j^+, \sigma_j^-, \sigma_j^z\right\}$, with raising and lowering operators $\sigma_j^\pm = \frac{\sigma_j^x \pm i\sigma_j^y}{\sqrt{2}}$ that breaks $U(1)$ symmetry (see the Supplementary material for details). Consequently,

$$\Delta S_A^{(2)}(t) = \log \frac{\sum_{\boldsymbol{\mu}} |\langle P^{\boldsymbol{\mu}} \rangle_t|^2}{\sum_{\boldsymbol{\mu}, [P^{\boldsymbol{\mu}}, Q_A]=0} |\langle P^{\boldsymbol{\mu}} \rangle_t|^2}, \tag{6}$$

where the projections in $\rho_{A,Q}$ correspond to discarding the operator strings anti-commute with Q_A. Subsequently, the calculation of EA reduces to evaluating the expectation values of P^μ. In the long time limit $t \to \infty$, we have

$$\Delta S_A^{(2)}(t \to \infty, \theta) \approx \log \left(1 + \left(\frac{1 + \cos^2(\theta)}{2}\right)^{N-2N_A} - \left(\frac{1 + \cos^2(\theta)}{2}\right)^{N-N_A}\right), \tag{7}$$

which indicates that the long-time EA converges to zero in the thermodynamic limit (see Fig. 3). The late-time EA behaviors with varying tilt angle θ encode the information of both symmetry

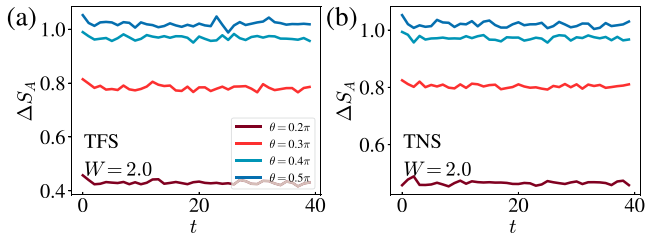

Fig. 2. EA dynamics in the Anderson localization phase with $V = 0$ and $W = 2.0$ with initial (a) TFS and (b) TNS. Here, $N = 80$ and $N_A = 10$.

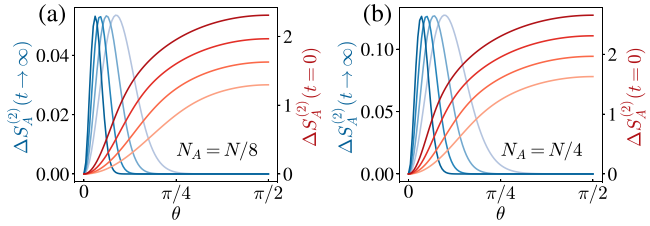

Fig. 3. The Rényi-2 EA $\Delta S_A^{(2)}$ of the initial state (red) and in the long time limit (blue). System sizes $N = [32, 64, 128, 256]$ are represented with darker colors for larger N, and the subsystem sizes are set to $N_A = N/8$ and $N/4$ for panels (a) and (b), respectively. A finite peak appears whose height remains unchanged as N increases (see the Supplementary material for more discussions) indicating a finite size crossover to persistently symmetry broken phase for small $\theta \sim \frac{1}{\sqrt{N}}$.

restoration and QME. On the one hand, zero late-time EA in the thermodynamic limit indicates symmetry restoration. On the other hand, the monotonic decreasing nature of late-time EA for a range of θ reflects the presence of QME in the middle times, as the order of EA with respect to θ is reversed compared to the initial monotonic increasing EA. As shown in Fig. 3, when $N_A < N/2$ and tilt angle θ is large, i.e., the initial state is more U(1) asymmetric, the late-time Rényi-2 EA approaches zero and thus the symmetry can be restored in the MBL regime. However, when θ is sufficiently small, i.e., the initial state is more U(1) symmetric, the late-time Rényi-2 EA is finite and the height of the peak shown in Fig. 3a, b stays the same with increasing system size N while its position scales as $\theta \sim \frac{1}{\sqrt{N}}$, implying a finite-size crossover for persistent symmetry broken phases. Meanwhile, the late-time monotonic decreasing EA with respect to θ for $N_A < N/2$ indicates the emergence of QME. Notably, the late-time EA results for the effective MBL model are the same for different Hamiltonian parameters and different initial product states, and also quantitatively coincide with the late-time EA results in the quantum chaotic case from TFS [40].

Furthermore, we directly simulate the $\Delta S_A^{(2)}$ dynamics under the quench of the effective Hamiltonian in Eq. (4). As shown in Fig. 4, the theoretical values in the long time limit agree well with the numerical results. More importantly, the dynamical behaviors of the effective model are qualitatively consistent with the actual dynamics, including the persistent symmetry breaking manifested as nonzero late-time EA in finite-size systems and the presence of QME regardless of the type of initial states.

Unlike quantum chaotic quench from TFS and MBL quench from generic tilted product states, late-time EA after quantum chaotic quench from other tilted product states beyond ferromagnetic states exhibits distinct behaviors – the symmetry can always be restored without finite-size symmetry breaking peak in small θ (see the Supplementary material for details). The similarity between MBL quench from generic tilted product states with quantum chaotic quench from TFS as well as the difference between

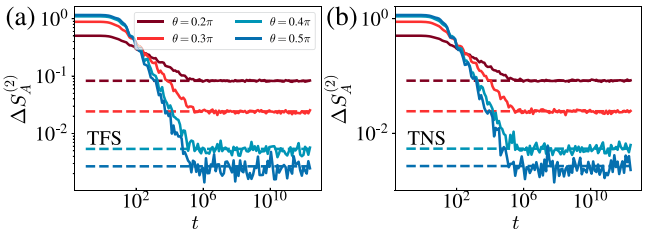

Fig. 4. Rényi-2 EA dynamics $\Delta S_A^{(2)}(t)$ of the effective model in Eq. (4) with $h = 10.0, J = 0.5$ and $\xi = 1.0$. The system size is set to $N = 14$ with subsystem size $N_A = 3$. The initial states of (a) and (b) are TFS and TNS respectively. Solid lines denote numerical results, while dashed lines indicate the theoretical late-time predictions.

quantum chaotic quench from TFS and other tilted product states can be understood in a unified framework. The key factor is the Hilbert space dimension accessible by the initial product state. In the effective MBL model cases and ferromagnetic initial states cases with charge conservation, the accessible Hilbert space dimensions are both $O(1)$ while for other product states with a fixed ratio of charge under chaotic evolution, the accessible Hilbert space dimensions grows exponentially. Therefore, in the former case, the effective accessible Hilbert space dimension is still severely restricted with small tilt angles θ, rendering persistent symmetry breaking in finite size. On the contrary, in the latter case, the exponentially large Hilbert space dimension yields sufficient relaxation to equilibrium for all θ. This framework is also consistent with the mechanism for QME in chaotic systems – small charge sectors are hard to thermalize and equilibrate only very slowly.

4. Discussion and conclusion

In this work, we investigate the U(1) symmetry restoration in the many-body localization regime. The U(1) symmetry can be restored in the MBL regime on an exponential time scale even though MBL forbids thermalization. Interestingly, the QME persists in the MBL regime regardless of the choice of the initial tilted product states, which is distinct from the cases in the integrable and chaotic systems. Theoretically, we derive the analytical expressions of the entanglement asymmetry for the effective MBL model in the long time limit, which are shown to be independent of the initial product states and consistent with the numerical simulation. Moreover, when the system is finite in size, the late-time subsystem symmetry cannot be fully restored and the EA remains finite when the tilt angle θ is sufficiently small but decays to zero when the tilt angle θ is large. Such late-time behaviors are reminiscent of chaotic quench from TFS, and the opposite monotonicity for EA with respect to θ between late time and early time supports the presence of the QME.

The mechanism underlying the QME in the MBL regime is fundamentally different from that in integrable and chaotic systems, characterized by different QME timescales and initial state dependence. Using the effective model, we have provided a theoretical analysis of the symmetry restoration in the MBL regime stabilized by the strong disorder. One interesting future direction is to study symmetry restoration in other types of MBL systems [111–128]. More importantly, this work not only offers a meaningful simulation task for current quantum devices [129,130] but also introduces a new and powerful criterion for the existence of the MBL phase: QME exists starting from TNS. Compared to the logarithmic growth of entanglement entropy, our new qualitative metric requires a much shorter evolution time and does not suffer from the subtlety induced by fitting choices.

Conflict of interest

The authors declare that they have no conflict of interest.

Acknowledgments

This work was supported in part by the National Natural Science Foundation of China (12347107 and 12334003), the MOSTC (2021YFA1400100), and the New Cornerstone Science Foundation through the Xplorer Prize. Hao-Kai Zhang is supported by the Postdoctoral Fellowship Program and China Postdoctoral Science Foundation (BX20250169). Shi-Xin Zhang acknowledges the support from Innovation Program for Quantum Science and Technology (2024ZD0301700) and the start-up grant at IOP-CAS. Shuai Yin is supported by the National Natural Science Foundation of China (12075324 and 12222515) and the Science and Technology Projects in Guangdong Province (2021QN02X561). Shuo Liu's work at Princeton University was supported by the Gordon and Betty Moore Foundation (GBMF8685) toward the Princeton Theory Program, the Gordon and Betty Moore Foundation's EPiQS Initiative (GBMF11070), the Office of Naval Research (N00014-20–1-2303), the Global Collaborative Network Grant at Princeton University, the Simons Investigator Grant (404513), the BSF Israel US foundation (2018226), the NSF-MERSEC (MERSEC DMR 2011750), the Simons Collaboration on New Frontiers in Superconductivity, and the Schmidt Foundation at the Princeton University.

Author contributions

Hong Yao and Shi-Xin Zhang conceived and designed the project. Shuo Liu, Hao-Kai Zhang, and Shi-Xin Zhang performed numerical simulations and contributed theoretical analysis. All authors contributed to discussions and production of the manuscript.

Appendix A. Supplementary material

Supplementary data to this article can be found online at https://doi.org/10.1016/j.scib.2025.10.017.

References

[1] Mpemba EB, Osborne DG. Cool? Phys Educ 1969;4:172.
[2] Lasanta A, Vega Reyes F, Prados A, et al. When the hotter cools more quickly: Mpemba effect in granular fluids. Phys Rev Lett 2017;119:148001.
[3] Lu Z, Raz O. Nonequilibrium thermodynamics of the markovian Mpemba effect and its inverse. Proc Natl Acad Sci USA 2017;114:5083–8.
[4] Klich I, Raz O, Hirschberg O, et al. Mpemba index and anomalous relaxation. Phys Rev X 2019;9:021060.
[5] Kumar A, Bechhoefer J. Exponentially faster cooling in a colloidal system. Nature 2020;584:64–8.
[6] Bechhoefer J, Kumar A, Chétrite R. A fresh understanding of the Mpemba effect. Nat Rev Phys 2021;3:534–5.
[7] Kumar A, Chétrite R, Bechhoefer J. Anomalous heating in a colloidal system. Proc Natl Acad Sci USA 2022;119:e2118484119.
[8] Walker MR, Vucelja M. Mpemba effect in terms of mean first passage time. arXiv:2212.07496, 2023.
[9] Walker MR, Bera S, Vucelja M. Optimal transport and anomalous thermal relaxations. arXiv:2307.16103, 2023.
[10] Bera S, Walker MR, Vucelja M. Effect of dynamics on anomalous thermal relaxations and information exchange. arXiv:2308.04557, 2023.
[11] Teza G, Yaacoby R, Raz O. Relaxation shortcuts through boundary coupling. Phys Rev Lett 2023;131:017101.
[12] Malhotra I, Löwen H. Double Mpemba effect in the cooling of trapped colloids. J Chem Phys 2024;161:164903.
[13] Nava A, Fabrizio M. Lindblad dissipative dynamics in the presence of phase coexistence. Phys Rev B 2019;100:125102.
[14] Chatterjee AK, Takada S, Hayakawa H. Multiple quantum Mpemba effect: exceptional points and oscillations. Phys Rev A 2024;110:022213.
[15] Chatterjee AK, Takada S, Hayakawa H. Quantum Mpemba effect in a quantum dot with reservoirs. Phys Rev Lett 2023;131:080402.
[16] Kochsiek S, Carollo F, Lesanovsky I. Accelerating the approach of dissipative quantum spin systems towards stationarity through global spin rotations. Phys Rev A 2022;106:012207.
[17] Carollo F, Lasanta A, Lesanovsky I. Exponentially accelerated approach to stationarity in markovian open quantum systems through the Mpemba effect. Phys Rev Lett 2021;127:060401.
[18] Ivander F, Anto-Sztrikacs N, Segal D. Hyperacceleration of quantum thermalization dynamics by bypassing long-lived coherences: an analytical treatment. Phys Rev E 2023;108:014130.
[19] Aharony Shapira S, Shapira Y, Markov J, et al. Inverse Mpemba effect demonstrated on a single trapped ion qubit. Phys Rev Lett 2024;133:010403.
[20] Strachan DJ, Purkayastha A, Clark SR. Non-markovian quantum Mpemba effect. Phys Rev Lett 2025;134:220403.
[21] Zhang J, Xia G, Wu CW, et al. Observation of quantum strong Mpemba effect. Nat Commun 2025;16:301.
[22] Wang X, Wang J. Mpemba effects in nonequilibrium open quantum systems. Phys Rev Res 2024;6:033330.
[23] Moroder M, Culhane O, Zawadzki K, et al. Thermodynamics of the quantum Mpemba effect. Phys Rev Lett 2024;133:140404.
[24] Manikandan SK. Equidistant quenches in few-level quantum systems. Phys Rev Res 2021;3:043108.
[25] Nava A, Egger R. Mpemba effects in open nonequilibrium quantum systems. Phys Rev Lett 2024;133:136302.
[26] Srivastav A, Pandey V, Mohan B, et al. Family of exact and inexact quantum speed limits for completely positive and trace-preserving dynamics. arXiv:2406.08584, 2024.
[27] Xu M, Wei Z, Jiang XP, et al. Expedited thermalization dynamics in incommensurate systems. arXiv:2505.03645, 2025.
[28] Wei Z, Xu M, Jiang XP, et al. Quantum Mpemba effect in dissipative spin chains at criticality. arXiv:2508.18906, 2025.
[29] Ares F, Murciano S, Calabrese P. Entanglement asymmetry as a probe of symmetry breaking. Nat Commun 2023;14:2036.
[30] Ares F, Calabrese P, Murciano S. The quantum Mpemba effects. Nat Rev Phys 2025;7:451–60.
[31] Yu H, Liu S, Zhang SX. Quantum Mpemba effects from symmetry perspectives. AAPPS Bull 2025;35:17.
[32] Murciano S, Ares F, Klich I, et al. Entanglement asymmetry and quantum Mpemba effect in the xy spin chain. J Stat Mech 2024;2024:013103.
[33] Ares F, Murciano S, Vernier E, et al. Lack of symmetry restoration after a quantum quench: an entanglement asymmetry study. SciPost Phys 2023;15:089.
[34] Chalas K, Ares F, Rylands C, et al. Multiple crossings during dynamical symmetry restoration and implications for the quantum Mpemba effect. J Stat Mech 2024;2024:103101.
[35] Bertini B, Klobas K, Collura M, et al. Dynamics of charge fluctuations from asymmetric initial states. Phys Rev B 2024;109:184312.
[36] Rylands C, Klobas K, Ares F, et al. Microscopic origin of the quantum Mpemba effect in integrable systems. Phys Rev Lett 2024;133:010401.
[37] Yamashika S, Ares F, Calabrese P. Entanglement asymmetry and quantum Mpemba effect in two-dimensional free-fermion systems. Phys Rev B 2024;110:085126.
[38] Caceffo F, Murciano S, Alba V. Entangled multiplets, asymmetry, and quantum Mpemba effect in dissipative systems. J Stat Mech 2024;2024:063103.
[39] Ares F, Vitale V, Murciano S. Quantum Mpemba effect in free-fermionic mixed states. Phys Rev B 2025;111:104312.
[40] Liu S, Zhang HK, Yin S, et al. Symmetry restoration and quantum Mpemba effect in symmetric random circuits. Phys Rev Lett 2024;133:140405.
[41] Turkeshi X, Calabrese P, De Luca A. Quantum Mpemba effect in random circuits. Phys Rev Lett 2025;135:040403.
[42] Foligno A, Calabrese P, Bertini B. Nonequilibrium dynamics of charged dual-unitary circuits. PRX Quantum 2025;6:010324.
[43] Yu H, Li ZX, Zhang SX. Symmetry breaking dynamics in quantum many-body systems. arXiv:2501.13459, 2025.
[44] Yu H, Hu JP, Zhang SX. Quantum pontus-Mpemba effects in real and imaginary-time dynamics. arXiv:2509.01960, 2025.
[45] Chang WX, Yin S, Zhang SX, et al. Imaginary-time Mpemba effect in quantum many-body systems. arXiv:2409.06547, 2024.
[46] Joshi LK, Franke J, Rath A, et al. Observing the quantum Mpemba effect in quantum simulations. Phys Rev Lett 2024;133:010402.
[47] Xu Y, Fang CP, Chen BJ, et al. Observation and modulation of the quantum Mpemba effect on a superconducting quantum processor. arXiv:2508.07707, 2025.
[48] Klobas K, Rylands C, Bertini B. Translation symmetry restoration under random unitary dynamics. Phys Rev B 2025;111:L140304.
[49] Nandkishore R, Huse DA. Many-body localization and thermalization in quantum statistical mechanics. Annu Rev Condens Matter Phys 2015;6:15–38.
[50] Altman E, Vosk R. Universal dynamics and renormalization in many-body-localized systems. Annu Rev Condens Matter Phys 2015;6:383–409.
[51] Abanin DA, Papić Z. Recent progress in many-body localization. Ann Phys 2017;529:1700169.
[52] Abanin DA, Altman E, Bloch I, et al. Colloquium: many-body localization, thermalization, and entanglement. Rev Mod Phys 2019;91:021001.
[53] Alet F, Laflorencie N. Many-body localization: an introduction and selected topics. C R Phys 2018;19:498–525.
[54] Sierant P, Lewenstein M, Scardicchio A, et al. Many-body localization in the age of classical computing. Rep Prog Phys 2025;88:026502.

[55] Bera S, De Tomasi G, Weiner F, et al. Density propagator for many-body localization: finite-size effects, transient subdiffusion, and exponential decay. Phys Rev Lett 2017;118:196801.
[56] Weiner F, Evers F, Bera S. Slow dynamics and strong finite-size effects in many-body localization with random and quasiperiodic potentials. Phys Rev B 2019;100:104204.
[57] Šuntajs J, Bonča J, Prosen T, et al. Quantum chaos challenges many-body localization. Phys Rev E 2020;102:062144.
[58] Šuntajs J, Bonča J, Prosen T, et al. Ergodicity breaking transition in finite disordered spin chains. Phys Rev B 2020;102:064207.
[59] Panda RK, Scardicchio A, Schulz M, et al. Can we study the many-body localisation transition? Europhys Lett 2020;128:67003.
[60] Kiefer-Emmanouilidis M, Unanyan R, Fleischhauer M, et al. Evidence for unbounded growth of the number entropy in many-body localized phases. Phys Rev Lett 2020;124:243601.
[61] Kiefer-Emmanouilidis M, Unanyan R, Fleischhauer M, et al. Slow delocalization of particles in many-body localized phases. Phys Rev B 2021;103:024203.
[62] Sierant P, Zakrzewski J. Challenges to observation of many-body localization. Phys Rev B 2022;105:224203.
[63] Morningstar A, Colmenarez L, Khemani V, et al. Avalanches and many-body resonances in many-body localized systems. Phys Rev B 2022;105:174205.
[64] Sels D, Polkovnikov A. Thermalization of dilute impurities in one-dimensional spin chains. Phys Rev X 2023;13:011041.
[65] Žnidarič M, Prosen T, Prelovšek P. Many-body localization in the heisenberg xxz magnet in a random field. Phys Rev B 2008;77:064426.
[66] Pal A, Huse DA. Many-body localization phase transition. Phys Rev B 2010;82:174411.
[67] Iyer S, Oganesyan V, Refael G, et al. Many-body localization in a quasiperiodic system. Phys Rev B 2013;87:134202.
[68] Deutsch JM. Quantum statistical mechanics in a closed system. Phys Rev A 1991;43:2046–9.
[69] Srednicki M. Chaos and quantum thermalization. Phys Rev E 1994;50:888–901.
[70] D'Alessio L, Kafri Y, Polkovnikov A, et al. From quantum chaos and eigenstate thermalization to statistical mechanics and thermodynamics. Adv Phys 2016;65:239–362.
[71] Rigol M, Dunjko V, Olshanii M. Thermalization and its mechanism for generic isolated quantum systems. Nature 2008;452:854–8.
[72] Deutsch JM. Eigenstate thermalization hypothesis. Rep Prog Phys 2018;81:082001.
[73] Bardarson JH, Pollmann F, Moore JE. Unbounded growth of entanglement in models of many-body localization. Phys Rev Lett 2012;109:017202.
[74] Serbyn M, Papić Z, Abanin DA. Universal slow growth of entanglement in interacting strongly disordered systems. Phys Rev Lett 2013;110:260601.
[75] Deng DL, Li X, Pixley JH, et al. Logarithmic entanglement lightcone in many-body localized systems. Phys Rev B 2017;95:024202.
[76] Huang Y, Zhang YL, Chen X. Out-of-time-ordered correlators in many-body localized systems. Ann Phys 2017;529:1600318.
[77] Fan R, Zhang P, Shen H, et al. Out-of-time-order correlation for many-body localization. Sci Bull 2017;62:707–11.
[78] Chen X, Zhou T, Huse DA, et al. Out-of-time-order correlations in many-body localized and thermal phases. Ann Phys 2017;529:1600332.
[79] Bañuls MC, Yao NY, Choi S, et al. Dynamics of quantum information in many-body localized systems. Phys Rev B 2017;96:174201.
[80] Chen YQ, Liu S, Zhang SX. Subsystem information capacity in random circuits and hamiltonian dynamics. Quantum 2025;9:1783.
[81] Serbyn M, Papić Z, Abanin DA. Local conservation laws and the structure of the many-body localized states. Phys Rev Lett 2013;111:127201.
[82] Huse DA, Nandkishore R, Oganesyan V. Phenomenology of fully many-body-localized systems. Phys Rev B 2014;90:174202.
[83] Lee M, Look TR, Lim SP, et al. Many-body localization in spin chain systems with quasiperiodic fields. Phys Rev B 2017;96:075146.
[84] Chandran A, Laumann CR. Localization and symmetry breaking in the quantum quasiperiodic ising glass. Phys Rev X 2017;7:031061.
[85] Nag S, Garg A. Many-body mobility edges in a one-dimensional system of interacting fermions. Phys Rev B 2017;96:060203.
[86] Bar Lev Y, Kennes DM, Klöckner C, et al. Transport in quasiperiodic interacting systems: from superdiffusion to subdiffusion. Europhys Lett 2017;119:37003.
[87] Žnidarič M, Ljubotina M. Interaction instability of localization in quasiperiodic systems. Proc Natl Acad Sci USA 2018;115:4595–600.
[88] Crowley PJD, Chandran A, Laumann CR. Quasiperiodic quantum ising transitions in 1d. Phys Rev Lett 2018;120:175702.
[89] Setiawan F, Deng DL, Pixley JH. Transport properties across the many-body localization transition in quasiperiodic and random systems. Phys Rev B 2017;96:104205.
[90] Zhang SX, Yao H. Universal properties of many-body localization transitions in quasiperiodic systems. Phys Rev Lett 2018;121:206601.
[91] Zhang SX, Yao H. Strong and weak many-body localizations. arXiv:1906.00971, 2019.
[92] Liu S, Zhang SX, Hsieh CY, et al. Probing many-body localization by excited-state variational quantum eigensolver. Phys Rev B 2023;107:024204.
[93] Falcão PRN, Aramthottil AS, Sierant P, et al. Many-body localization crossover is sharper in a quasiperiodic potential. Phys Rev B 2024;110:184209.
[94] Luitz DJ, Laflorencie N, Alet F. Many-body localization edge in the random-field heisenberg chain. Phys Rev B 2015;91:081103.
[95] Sierant P, Zakrzewski J. Level statistics across the many-body localization transition. Phys Rev B 2019;99:104205.
[96] Fossati M, Ares F, Dubail J, et al. Entanglement asymmetry in cft and its relation to non-topological defects. J High Energy Phys 2024;2024:59.
[97] Chen M, Chen HH. Rényi entanglement asymmetry in (1+1)-dimensional conformal field theories. Phys Rev D 2024;109:065009.
[98] Capizzi L, Mazzoni M. Entanglement asymmetry in the ordered phase of many-body systems: the ising field theory. J High Energy Phys 2023;2023:144.
[99] Capizzi L, Vitale V. A universal formula for the entanglement asymmetry of matrix product states. J Phys A 2024;57:45LT01.
[100] Ares F, Murciano S, Piroli L, et al. Entanglement asymmetry study of black hole radiation. Phys Rev D 2024;110:L061901.
[101] Khor BJJ, Kürkçüoğlu DM, Hobbs TJ, et al. Confinement and kink entanglement asymmetry on a quantum ising chain. Quantum 2024;8:1462.
[102] Benini F, Godet V, Singh AH. Entanglement asymmetry in conformal field theory and holography. Prog Theor Exp Phys 2025;2025:063B05.
[103] Zhang SX, Allcock J, Wan ZQ, et al. Tensorcircuit: a quantum software framework for the NISQ era. Quantum 2023;7:912.
[104] Weinberg P, Bukov M. Quspin: a python package for dynamics and exact diagonalisation of quantum many body systems part I: spin chains. SciPost Phys 2017;2:003.
[105] Weinberg P, Bukov M. Quspin: a python package for dynamics and exact diagonalisation of quantum many body systems. part II: bosons, fermions and higher spins. SciPost Phys 2019;7:020.
[106] Evers F, Modak I, Bera S. Internal clock of many-body delocalization. Phys Rev B 2023;108:134204.
[107] Imbrie JZ. On many-body localization for quantum spin chains. J Stat Phys 2016;163:998–1048.
[108] Imbrie JZ. Diagonalization and many-body localization for a disordered quantum spin chain. Phys Rev Lett 2016;117:027201.
[109] Imbrie JZ, Ros V, Scardicchio A. Local integrals of motion in many-body localized systems. Ann Phys 2017;529:1600278.
[110] Rademaker L, Ortuño M, Somoza AM. Many-body localization from the perspective of integrals of motion. Ann Phys 2017;529:1600322.
[111] Levi E, Heyl M, Lesanovsky I, et al. Robustness of many-body localization in the presence of dissipation. Phys Rev Lett 2016;116:237203.
[112] Medvedyeva MV, Prosen T, Žnidarič M. Influence of dephasing on many-body localization. Phys Rev B 2016;93:094205.
[113] Sierant P, Zakrzewski J. Many-body localization of bosons in optical lattices. New J Phys 2018;20:043032.
[114] Hamazaki R, Kawabata K, Ueda M. Non-hermitian many-body localization. Phys Rev Lett 2019;123:090603.
[115] Schulz M, Hooley CA, Moessner R, et al. Stark many-body localization. Phys Rev Lett 2019;122:040606.
[116] van Nieuwenburg E, Baum Y, Refael G. From bloch oscillations to many-body localization in clean interacting systems. Proc Natl Acad Sci USA 2019;116:9269–74.
[117] Mu S, Lee CH, Li L, et al. Emergent fermi surface in a many-body non-hermitian fermionic chain. Phys Rev B 2020;102:081115.
[118] Zhai LJ, Yin S, Huang GY. Many-body localization in a non-hermitian quasiperiodic system. Phys Rev B 2020;102:064206.
[119] Khemani V, Hermele M, Nandkishore R. Localization from hilbert space shattering: from theory to physical realizations. Phys Rev B 2020;101:174204.
[120] Bhakuni DS, Sharma A. Entanglement and thermodynamic entropy in a clean many-body-localized system. J Phys Condens Matter 2020;32:255603.
[121] Heußen S, White CD, Refael G. Extracting many-body localization lengths with an imaginary vector potential. Phys Rev B 2021;103:064201.
[122] Doggen EVH, Gornyi IV, Polyakov DG. Stark many-body localization: evidence for hilbert-space shattering. Phys Rev B 2021;103:L100202.
[123] Chen YQ, Zhang SX, Zhang S. Non-markovianity benefits quantum dynamics simulation. arXiv:2311.17622, 2023.
[124] Liu S, Zhang SX, Hsieh CY, et al. Discrete time crystal enabled by stark many-body localization. Phys Rev Lett 2023;130:120403.
[125] Sierant P, Lewenstein M, Scardicchio A, et al. Stability of many-body localization in floquet systems. Phys Rev B 2023;107:115132.
[126] Sarkar S, Buča B. Protecting coherence from the environment via stark many-body localization in a quantum-dot simulator. Quantum 2024;8:1392.
[127] Aramthottil AS, Sierant P, Lewenstein M, et al. Phenomenology of many-body localization in bond-disordered spin chains. Phys Rev Lett 2024;133:196302.
[128] Jian SK, Yao H. Solvable sachdev-ye-kitaev models in higher dimensions: from diffusion to many-body localization. Phys Rev Lett 2017;119:206602.
[129] Mi X, Ippoliti M, Quintana C, et al. Time-crystalline eigenstate order on a quantum processor. Nature 2022;601:531–6.
[130] Schreiber M, Hodgman SS, Bordia P, et al. Observation of many-body localization of interacting fermions in a quasirandom optical lattice. Science 2015;349:842–5.